MORE DETAILS ON THE INTERNAL MAGNETIC FIELD BY SEPARATE FIELD MODELS REFERRED TO THE EARTH´S GROUND AND TO DIFFERENT BALLOON AND SATELLITE ALTITUDES

Wigor A. Webers

Helmholtz-Zentrum Potsdam, Deutsches GeoForschungsZentrum, German, E-mail: wigor@gfz-potsdam.de

ABSTRACT

The usual internal magnetic field models in the form of the spherical harmonic expansions (SHA) are calculated from multi-altitude magnetic observations (ground, balloon and satellite altitudes). According to the author´s paper [1] from the mathematics of modelling the internal magnetic field there results that the different physical properties of magnetic field data in dependence on the altitudes cause that only a mean internal magnetic field model is derived when field data from different altitudes are commonly used without any reasonable potential field continuation procedure.
Consequently, the ill-posed problems of upward and downward potential field continuations must be approximated in an appropriate way by considering e.g. recorded field data at different altitudes. The procedure derived is based on the altitude dependence of the internal magnetic field as a potential field that decreases with increasing distances from the Earth´s body so that the continuation procedure uses this dependence as regularizing criterion.

When from now on magnetic field data are available simultaneously for definite time intervals from different altitudes (ground, balloon and satellites) as e.g. for the planned SWARM project than separate internal magnetic field models referred to different altitudes can be calculated and they can be compared to each-other in combination with approximated upward and downward field continuations according to the published procedure of the author [1]). The paper here gives model calculations as numerical examples that demonstrate how efficient this separate modelling shows model details in dependence on altitudes .More details on the internal magnetic field are of special importance when small field constituents as the crustal contributions are studied.

1. INTRODUCTION

The magnetic field recorded at irregularly distributed observatories and stations, contains internal and external field contributions. The internal includes components dominated by the Earth's main or core field, as well as relatively smaller contributions from the Earth's mantle and lithosphere.
These magnetic field constituents are differently represented in observations taken at the Earth's surface and satellite altitude due to the different measurement errors and mathematical properties. The external magnetic field effects, for example, tend to contaminate the lithospheric components of the internal magnetic field much more severely at satellite altitude than at the Earth's surface. Consequently, field models of the two data sets will reflect fundamentally different source effects.
However, imposing effective constraints on the convergence behaviour in the downward continuation of satellite altitude model can improve the utility of the model for representing the internal field at the Earth's surface.

2. MATHEMATICAL FORMULATION

From potential field theory, the internal magnetic field of the Earth may be represented as the gradient of the potential V given by

$$B_{int} = - \nabla V, \tag{1}$$

where the spherical harmonic expansion (SHA) of the potential is

$$V = \sum_{n=1}^{N} \sum_{m=0}^{n} a \left(\frac{a}{r}\right)^{n+1} \left(g_n^m \cos m\lambda + h_n^m \sin m\lambda\right) P_n^m(\cos \vartheta) \tag{2}$$

and

(3)

(r, ϑ, λ) are the spherical polar coordinates

a is the radius of the Earth's surface (nominally 6,371.2 km)

Proc. '19th ESA Symposium on European Rocket and Balloon Programmes and Related Research, Bad Reichenhall, Germany, 7–11 June 2009 (ESA SP-671, September 2009)

P_n^m is a Schmidt quasi-normalized associated Legendre function of degree n and order m, and

g_n^m ; h_n^m are the Gauss coefficients.

In the space external to the source region (i.e. in free space), the potential V satisfies the Laplace equation, so that

$$\Delta V=0 \quad \text{for } r \geq a \tag{4}$$

In practice, the series expansion (2) is customarily referred to an Earth sphere of mean radius a = 6,371.3 km, or an ellipsoidial or other appropriate reference surface of the Earth.

The origionally infinite series expansion of Eq. (2) is approximated by the partial sum with the truncation index N.
Using the common index k instead of the indices n and m for the respective degree and order of the associated Legendre functions $P_n^m(\cos\vartheta)$ allows Eq. (2) to be expressed in terms of the orthogonal functional system $\{f_k\}$ and the coefficients $\{C_k\} = \{g_n^m ; h_n^m\}$.

(5)

$$\begin{aligned} f_1 &= a \cdot P_1^0 \\ f_2 &= a \cdot \cos\lambda P_1^1 \\ f_3 &= a \cdot \sin\lambda P_1^1 \\ f_4 &= a \cdot P_2^0 \end{aligned}$$

etc. and for all k = 1,2,..., N · (N+2).
The least squares method is applied to the derivatives of the potential V (Eq. (2)) for numerically calculating the Gauss coefficients $\{g_n^m ; h_n^m\} = \{C_k\}$ of the SHA field model.
For field components taken at the Earth´s surface the least squares determination references the functional system and Gauss coefficients to the sphere of radius $r=a$. However, the determination for observations taken at satellite altitude h are referenced to $r=a+h$. Obviously, the two data models are based on different functional systems and Gauss coefficients as can be seen by considering the first few terms of the potential (Eq. (2)) shown below.

for r = a	for r = a + h
n = 1	
$f_1 = a \cdot P_1^0$	$f_1 = a\left(1+\frac{h}{a}\right)^{-2} P_1^0$
$f_2 = a \cdot \cos\lambda P_1^1$	$f_2 = a\left(1+\frac{h}{a}\right)^{-2} \cos\lambda P_1^1$
$f_3 = a \cdot \sin\lambda P_1^1$	$f_3 = a\left(1+\frac{h}{a}\right)^{-2} \sin\lambda P_1^1$
n = 2	
$f_4 = a \cdot P_2^0$	$f_4 = a\left(1+\frac{h}{a}\right)^{-3} P_2^0$
$f_5 = a \cdot \cos\lambda P_2^1$	$f_5 = a\left(1+\frac{h}{a}\right)^{-3} \cos\lambda P_2^1$
$f_6 = a \cdot \sin\lambda P_2^1$	$f_6 = a\left(1+\frac{h}{a}\right)^{-3} \sin\lambda P_2^1$
$f_7 = a \cdot \cos2\lambda P_2^2$	$f_7 = a\left(1+\frac{h}{a}\right)^{-3} \cos2\lambda P_2^2$
$f_8 = a \cdot \sin2\lambda P_2^2$	$f_8 = a\left(1+\frac{h}{a}\right)^{-3} \sin2\lambda P_2^2$
n = 3	
$f_9 = a \cdot P_3^0$	$f_9 = a\left(1+\frac{h}{a}\right)^{-4} P_3^0$
$f_{10} = a \cdot \cos\lambda P_3^1$	$f_{10} = a\left(1+\frac{h}{a}\right)^{-4} \cos\lambda P_3^2$

etc. with the set of Gauss coefficients C_k and C'_k, respectively, being different due to the relevant functional systems.

Consequently, the different functional systems show clearly that finite internal magnetic field models of a definite truncation index N have significantly different properties in dependence on the altitude h of the balloon and the satellite, respectively. This can be used to receive more detailed information on the constituents of the internal magnetic field that differently reach the relevant altitudes.

Relating SHA field models to each other commonly involves upward or downward data continuation based on the ratios of the radii of the data reference surfaces. Downward continuation in particular is notoriously problematic and unstable, often yielding predictions with frequency components that are too high to have detected in the higher altitude data (e.g. [2], [1]). Taking into account the different convergence properties of the power series at the reference surface (e.g. [3]), however,

can improve the accuracy of field continuation over the first order predictions from the conventional ratios of the reference surface radii. This approach is especially useful for lithospheric anomaly predictions that require high accuracy predictions near the Earth´s surface of magnetic field models derived from balloon and satellite observations.

3. SHA MAGNETIC FIELD MODELS OF DIFFERENT ALTITUDES

To relate the different functional systems and their coefficients in Eqs. (5), note by the orthogonality of the system $\{f_k\}$ for the series expansion of the potential V (Eq. (2)) that it follows

$$\varphi_k = C_k \cdot f_k \tag{6}$$

where $\langle \varphi_i; \varphi_k \rangle = \frac{4\pi a^2}{2n+1} \cdot C_k^2$ for $i = k$

$= 0$ for $i \neq k$

and $k = 1,2,\ldots, N(N+2)$.

The two functional systems $\{f_k\}$ [cp. Eq.(5)] can be treated by comparing the contribution to a volume in the functional space being spanned by these functions that is made analogously to the geometrical understanding of the vector analysis where the volume of the k dimensional vector space is calculated by the GRAM determinant. The GRAM determinant has elements that are formed by the scalar products of the k vectors spanning the functional space.

Because of the orthogonality of the functional systems of Eq. (6), the GRAM determinant consists only of the non-zero-products $\langle \varphi_k, \varphi_k \rangle$ in the principal diagonal so that the product of the elements in the principal diagonal gives the volume. Therefore, it makes good sense to study the stepwise contribution of each $\langle \varphi_k , \varphi_k \rangle$, $k = 1, 2,\ldots , N (N + 2)$, to the volume G in functional dependence on the index k for both functional systems $\{f_k\}$ of Eqs. (5).

The functional dependence of G on the index k is an inherent mathematical invariant of the SHA model made by its functional system $\{f_k\}$ and relevant Gauss coefficients C_k that also characterizes its convergence behaviour. The SHA models are usefully compared in terms of $\log \psi (k)$ that is expressed approximately as the polynomial in k given by:

$$\log \psi (k) = c_o + c_1 k + c_2 k^2 + c_3 k^3 + \ldots \tag{7}$$

Eq. (7) is a considerably more comprehensive extension of the linear approximation of that in [4] that the author had developed to transform the Gauss coefficients $\{C_k\} = \{g_n^m ; h_n^m\}$ for the downward continuation of satellite altitude magnetic data.
Eq. (7) gives

$$C_{kreg}(n, k, C_k, r_1, r_2, \gamma, c_0^{(2)}) = \tag{8}$$

$$sign(C_k) \cdot \left[(2n+1) \cdot 10^{(1-\cos\gamma)\, c_0^{(2)} - (k + \frac{c_2}{c_1} k^2 + \frac{c_3}{c_1} k^3 + \ldots) \cdot \sin\gamma} \cdot \left(\frac{C_k^2}{2n+1} \cdot \left(\frac{r_1}{r_2} \right)^{2(n+1)} \right)^{\cos\gamma} \cdot \frac{(4\pi r_1^2)^{\cos\gamma}}{4\pi r_1^2} \right]^{\frac{1}{2}}$$

for $r_2 < r_1$ and $\gamma = \alpha_2 - \alpha_1$,

where

- r_1 is the radius of the satellite altitude reference surface
- r_2 is the radius of the ground reference surface
- α_1 is the slope of eq. (8) for the satellite altitude data; $c_1^{(1)} = \tan \alpha_1$
- α_2 is the slope of eq. (8) for the ground data; $c_1^{(2)} = \tan \alpha_2$
- γ is the difference of the slopes where $\gamma = \alpha_2 - \alpha_1$
- C_k are the Gauss coefficients for the satellite altitude data
- $c_o^{(2)}$ is the first (constant) term of eq. (8) for the ground data.

The *reg* index in the downward continued Gauss coefficients C_{kreg} [Eq. (8)] indicates the fact that the downward field continuation mathematically means an ill-posed inverse problem that is solved by a regularization process. Here, the regularization parameters γ, $c_0^{(2)}$, $c_j^{(1)}$ for $j = 0,1,2, \ldots$ [cp. Eqs. (7), (8)] have been derived from the inherent mathematical characteristics, i.e. the different convergence property at the ground in comparison to the satellite altitude. In this respect no further explanations are necessary, what the consequences of these regularizing parameters would mean.

4. CONCLUSIONS

Separate - but simultaneous in time - internal magnetic field models for concentric balloon and satellite altitudes in combination with mathematical field continuation procedures give essential details of the altitude dependence of the internal magnetic field.
In this way the field is split off for the different field constituents that shows which of them reach definite altitudes. These details will be of special interest when the field is discussed e.g. for its lithospheric sources.

.

In downward continuation the regularization of Eq. (8) increasingly dampens the effects of coefficients with increasing *k* indices. Consequently, the higher frequency terms of the SHA field model are numerically reduced so that the downward field continuation does not introduce shorter wavelengths of the internal magnetic field that cannot be observed at satellite altitude.
Consequently, when global internal magnetic field models of different altitudes are compared with upward and downward field continuations more details of the field become visible.

Moreover, the comparisons of separate field models (referred to their different reference surfaces) in combination with approximated field continuations – upward and downward – give an useful tool to separate internal and external magnetic field contributions to the recorded field data of different altitudes because the mathematical approximated continuation procedures only affect the mathematical forms and numerical values of the internal and the external contributions, respectively, but they do not change their principal contributions to their related altitudes.

5. REFERENCES

1. Webers, W. A. , *On different properties of internal magnetic field models at the Earth´s surface and at satellite altitudes*, J. Geodyn. 43, 239-247, 2007.
2. Anger, G., *Inverse problems in differential equations,* Akademie/Plenum Press, Berlin/London, 1990.
3. Knopp, K., *Theorie und Anwendung der unendlichen Reihen*, Springer Verlag, Berlin, 1922.
4. Webers, W. A., *Downward field continuation in combining satellite and ground-based internal magnetic field data*, J. Geodyn. 33, 101-116, 2002.

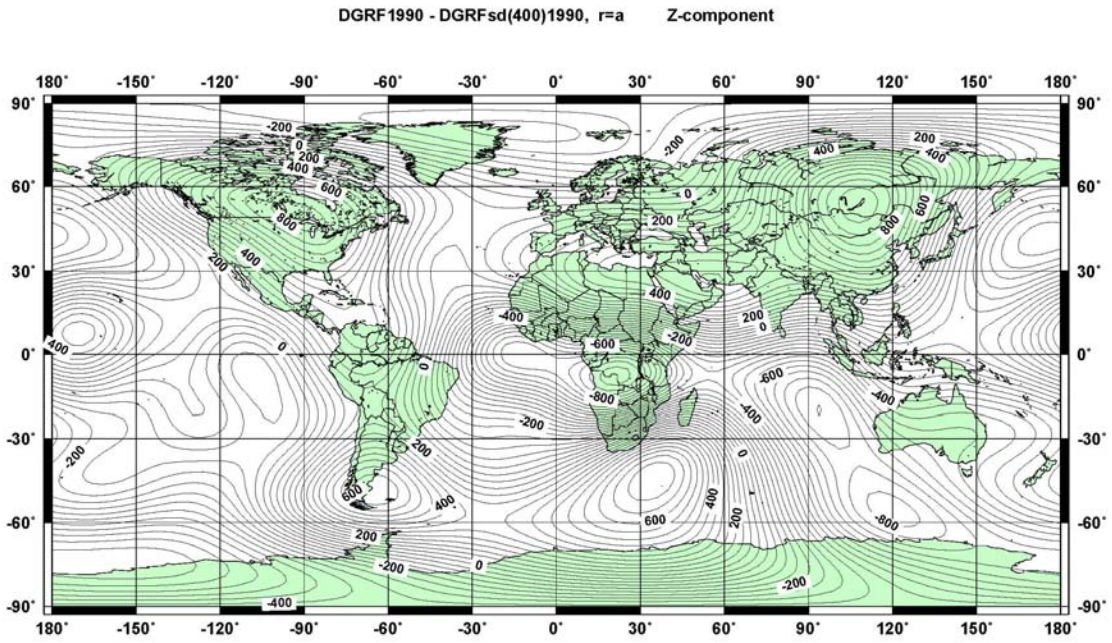

Fig. 1.
DGRF 1990: difference chart DGRF 1990 – DGRFsd (400) 1990, Z-component in nT:
DGRF 1990 mathematically upward continued to the satellite altitude of h = 400 km as DGRFs (400) 1990, downward continued to the ground as DGRFsd (400) 1990.

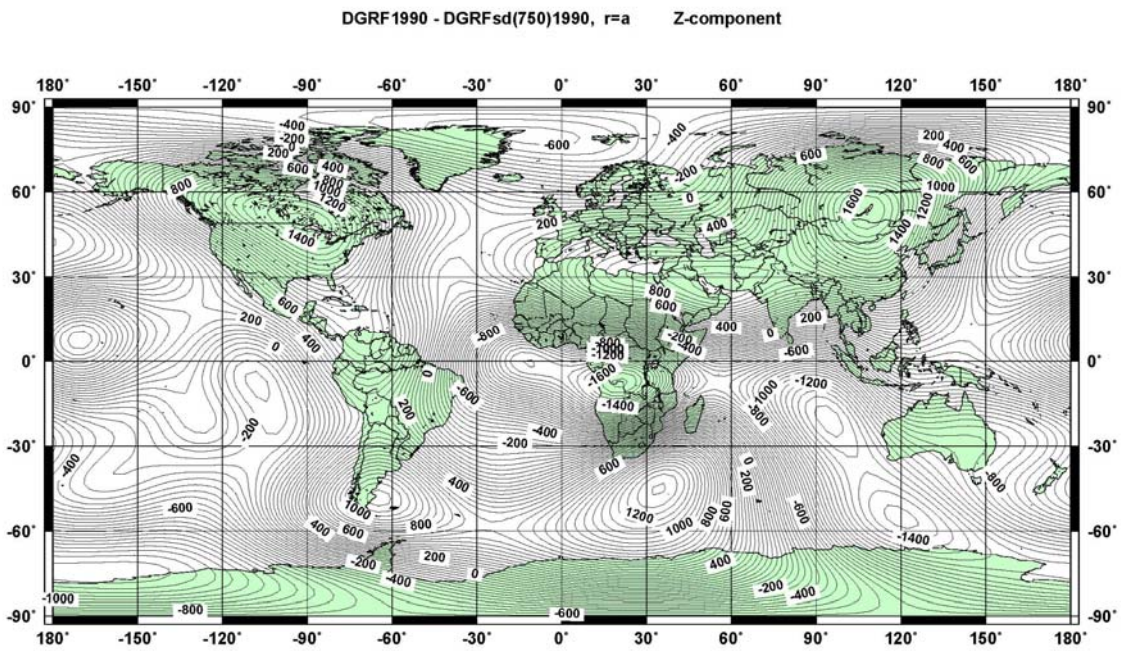

Fig. 2.
DGRF 1990: difference chart DGRF 1990 – DGRFsd (750) 1990, Z-component in nT:
DGRF 1990 mathematically upward continued to the satellite altitude of h = 750 km as DGRFs (750) 1990, downward continued to the ground as DGRFsd (750) 1990.

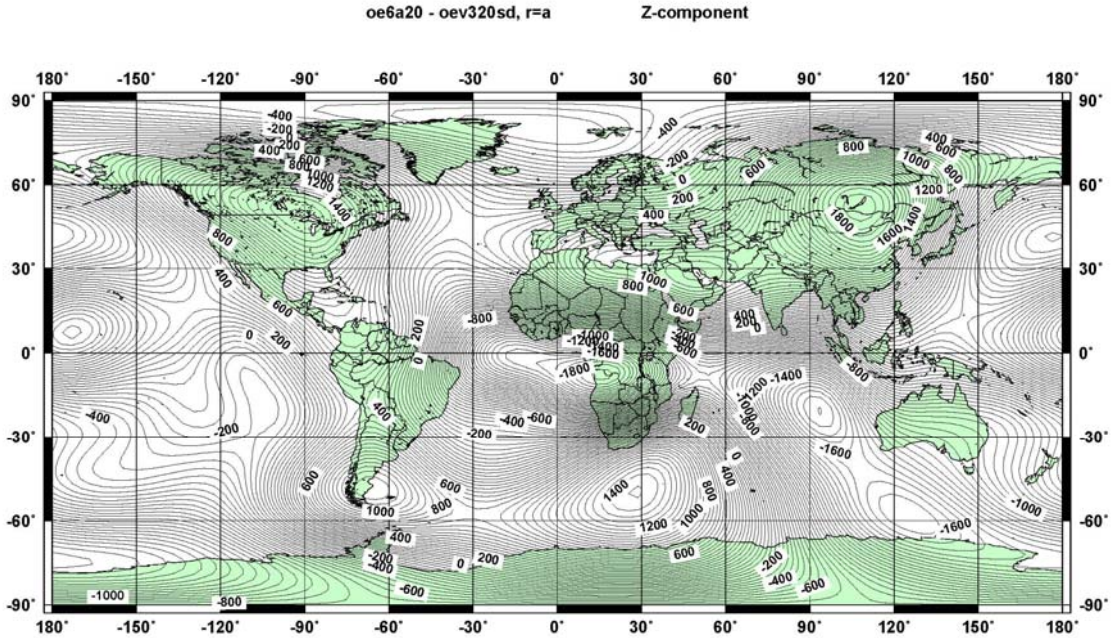

Fig. 3.
Oersted 6a: difference chart oe6a20 – oev320sd, Z-component in nT:
Oe6a mathematically upward continued to the satellite altitude of h = 750 km as oe6as, downward continued to the ground and referred to a polynomial of third degree (Eq. (7)) as oev320sd

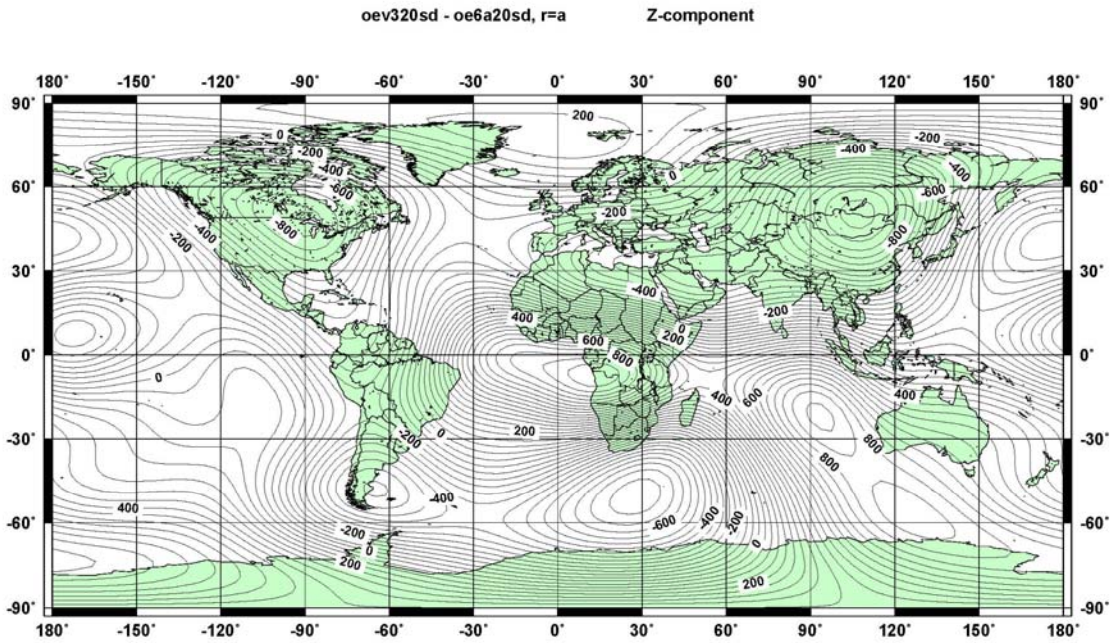

Fig. 4.
Oersted 6a: Difference chart oev320sd – oe6a20sd, Z- component:
Improvement of downward continuation according to Eq. (7) by a polynomial of third degree in comparison to that of first degree.